

Research Paper

Investigating the Design and Simulation of a Tunable Optical Filter Based on Photonic Crystal Using Selective Optofluidic Infiltration

Mahsa Bazargani¹, Behnaz Gharekhanlou^{*1}, Mehdi Banihashemi¹

¹ Department of Electrical Engineering, Central Tehran Branch, Islamic Azad University, Tehran, Iran

Received: 14 Sep. 2022

Revised: 11 Oct. 2022

Accepted: 17 Nov. 2022

Published: 20 Nov. 2022

Use your device to scan
and read the article
online



Keywords:

**Bandgap, Cavity,
Filter, Optofluidic,
Photonic crystal**

Abstract

In this paper an optical filter based on 2D hexagonal photonic crystals that is suitable for the third window of optical communications is proposed. The structure consists of two waveguides including one L4 resonant cavity created by removing 4 holes between them, and one L1 resonant cavity by removing 1 hole near the output waveguide; moreover, 8 holes around the L4 cavity had been selected for optofluidic infiltration within them. This structure is very flexible, and different wavelengths in the third telecommunication window can be chosen using selective optofluidic infiltration with different refractive indices. Simplicity in design, no need to change the size of the holes and separating the desired wavelengths by selecting different optofluidic infiltration materials are the main features of this study. The plane-wave expansion method (PWE) and the finite-difference time-domain method (FDTD) have been used to extract the photonic bandgap and study the behavior of the photonic structure, respectively.

Citation: Mahsa Bazargani, Behnaz Gharekhanlou, Mehdi Banihashemi. Investigating the Design and Simulation of a Tunable Optical Filter Based on Photonic Crystal Using Selective Optofluidic Infiltration. **Journal of Optoelectrical Nanostructures**. 2022; 7 (4): 66-79 **DOI** [10.30495/jopn.2022.29582.1248](https://doi.org/10.30495/jopn.2022.29582.1248)

***Corresponding author:** Bahnaz Gharekhanlou

Address: Department of Electrical Engineering, Central Tehran Branch, Islamic Azad University, Tehran, Iran. **Tell:** +982144600008 **Email:** beh.gharekhanlou@iauctb.ac.ir

1. INTRODUCTION

Photonic crystals (PCs) are flexible tools for realizing integrated optical circuits. These crystals have periodic structures in 1D, 2D, or 3D arrangements, and in each of which the refractive index of materials changes periodically. Due to the result of these periodicities, a region of wavelength may appear in which propagation in the lattice, namely the photonic bandgap (PBG), is forbidden [1]. This region is tunable by some parameters such as the dielectric constant of the materials, the lattice constant, and the size of holes or rods in the structure. By making some changes, such as point or line defects, the bandgap of the PC structures can be broken. Therefore, the type and place of the defects are very important to tune and control the wavelength of transmitted light [1–3]. By using defects in PBG, different elements can be designed, such as optical filters [4, 5], optical decoders [6], optical multiplexers [7], and optical demultiplexers [8, 9]. In general, the optical filters are the basic sections of many optical devices and there are two popular methods for designing and realizing optical filters, including the ring resonators, and the resonant cavities [10, 11]. Heretofore, in all of the structures that have been introduced by researchers, tuning and the selection of the desired wavelength has been done by changing the size of the radius of holes or rods at nano-scale in the structure, most of which are not possible in terms of fabrication. In this study, our goal is to provide a mechanism that does not require resizing the holes at the nanoscale. Therefore, a wavelength selection method was presented using selective optofluidic infiltration for cavity resonance. The numerical methods were used to analyze the behavior of electromagnetic waves and to extract the photonic bandgap region in the photonic crystal structure. One of the most popular numerical methods in the frequency domain is the plane-wave expansion method (PWE), which calculates frequency, polarization, symmetry, and field distribution of every eigenmode in the cavity as an infinite alternating structure [12]. However, the PWE is not an effective method for obtaining the normalized reflection output spectrum due to its limitation in terms of the steady-state calculation. Therefore, it is necessary to find another flexible method to solve more complex problems.

The finite-difference time-domain method (FDTD) is an accurate and flexible method for solving Maxwell equations and analyzing electromagnetic waves in the time domain; it allows us to determine the temporal behavior of the modes [13]. The Bandsolve simulation tool of RSoft software [14] has been employed for calculating and extracting PBG to implement the PWE and to study the

behavior of electromagnetic waves in the structure, the Fullwave simulation tool of RSoft software has been used to implement the FDTD.

The third telecommunication window (1530 nm- 1565 nm) has the least attenuation. Therefore, the design of the filter and other telecommunication devices is important in this window. In this study, our focus is on filter design in this wavelength range.

2. DESIGN PROCEDURE

In the current study, a hexagonal lattice structure of air holes was utilized in the dielectric slab. The structure is composed of three layers, SiO₂-Si-SiO₂. The 200 nm Si slab is located between two areas of SiO₂ of 80 nm and 1000 nm thickness at the top and bottom, respectively. We assigned an effective index of 2.8 to the dielectric material for 2D FDTD simulations. The array of holes in the X direction and the Z direction were 30 and 20, respectively. The lattice constant of the PC structure was 422 nm and the radius of the air hole was 115 nm. The contour map of the index profile of the structure is shown in Figure 1(a). The band structure diagram of this design had no defects along the frequency axis and was normalized by the lattice constant and the edges of the irreducible Brillouin zone (Γ , M, and K) as shown in Figure 1(b).

As can be seen, there was one photonic bandgap in transverse electric (TE) mode in the band structure diagram in the used range of $0.25 \leq a/\lambda \leq 0.3$. By choosing $a = 422$ nm, the PBG in TE mode, the range of wavelength would be $1406\text{nm} \leq \lambda \leq 1688\text{nm}$, which completely covers the third wavelength window (1530 nm-1565 nm) for optical communication. Then, in this research, all the simulations have been done in TE mode.

In this paper, the FDTD method was used to simulate the behavior of electromagnetic waves in the photonic crystal. The simulation of high-precision photonic crystal structures required three-dimensional calculations. However, with a very good approximation of the effective refractive index, the calculation of the structure can be performed in two dimensions because the three-dimensional calculation is very time-consuming and requires very powerful computer systems.

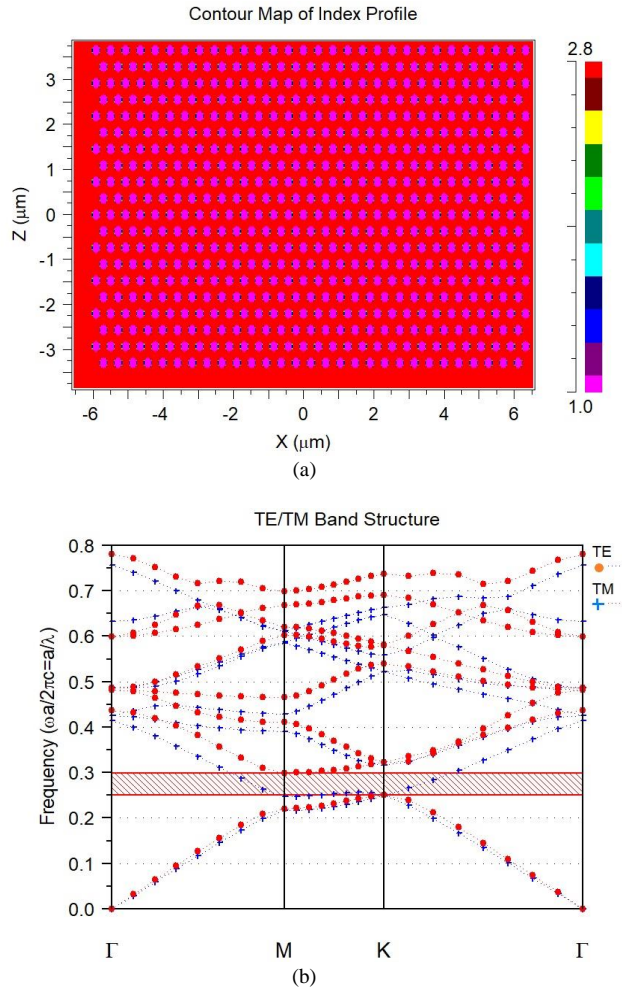


Fig. 1. (a) The contour map of index profile. (b) the band structure of diagram.

In the current design, the filter was composed of two optical waveguides as input and output waveguides, the L1 resonant cavity was near the output waveguide and the L4 (by removing 4 holes from the structure) resonant cavity was for separating the telecommunication's wavelength, as well as 8 holes around the L4 cavity. The air holes were infiltrated with optofluidic materials (see Figure.2).

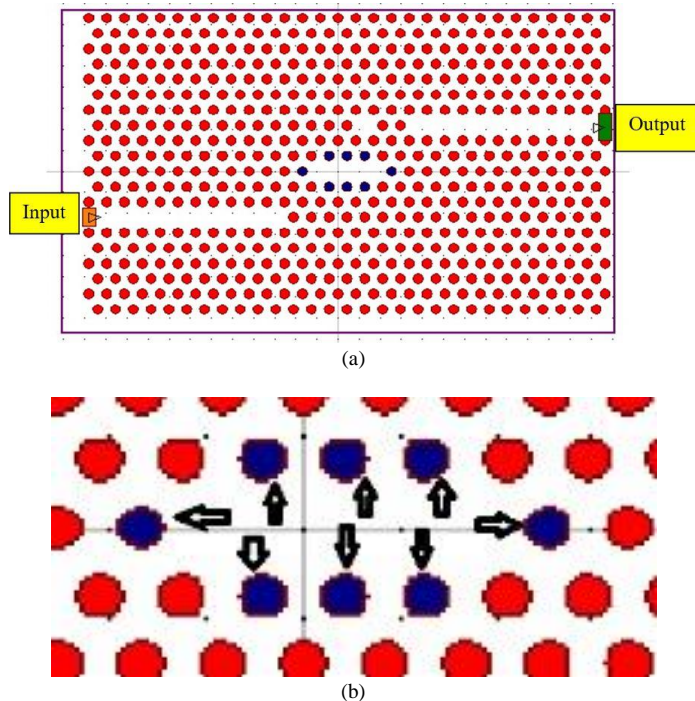


Fig. 2. (a) The filter structure, (b) more detail of marked holes around the L4 cavity infiltrated with optofluidic materials.

To select the appropriate L_x cavity ("x" is the number of holes removed) in the structure, the cavities of different lengths were tested, for example L2, L3, L4 and L5. The resonance's wavelength of the cavities depends on their size. The resonant wavelengths in the range of 1550 nm (central wavelength of third telecommunication window) are important for us. According to Figure 3, the resonant wavelengths from the L4 cavity were in the range of 1550 nm (by placing the source and monitor in the cavity place).

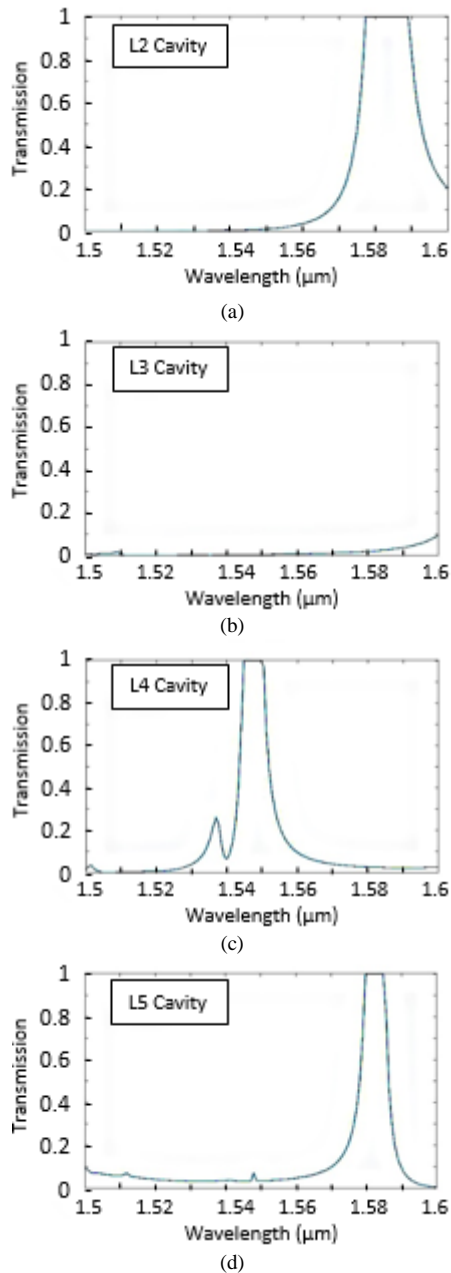


Fig. 3. The resonant wavelengths of the cavities without any fluid infiltration, (a) L2 cavity, (b) L3 cavity, (c) L4 cavity, (d) L5 cavity.

Up to this point, we found the size of the cavity, and because the distance between the monitor and the source from the cavity is important to determine the separated wavelength range, we moved the source to the input part. Figure 4 shows three states. State (1) shows the resonance wavelengths of the L4 cavity when the monitor and source were in the cavity site (no fluid has been infiltrated within the marked holes). State (2) shows the resonance wavelengths of the L4 cavity when the source was in the input of the circuit and the monitor was in the cavity site (no fluid has yet been infiltrated within the marked holes). As the refractive index of cavity increases, by optofluidic infiltration, the separated wavelengths move to higher wavelengths. State (3) shows the resonance wavelengths of the L4 cavity when the source was in the input of the circuit and the monitor was in the cavity site (the fluid has been infiltrated within the marked holes around L4 cavity with refractive index of 1.334).

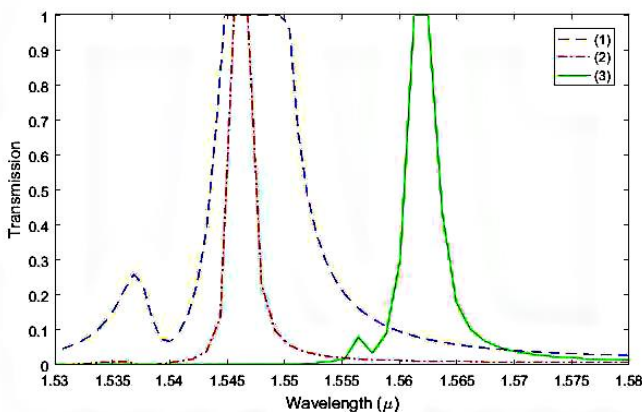


Fig. 4. The resonant wavelengths of the L4 cavity in three states:

State (1), the monitor and source were in the cavity site (no fluid has been infiltrated within the marked holes).

State (2), the source was in the input of the circuit and the monitor was in the cavity site (no fluid has yet been infiltrated within the marked holes).

State (3), the source was in the input of the circuit and the monitor was in the cavity site (the fluid has been infiltrated within the marked holes around L4 cavity with refractive index of 1.334).

To separate a single wavelength from several wavelengths located in the third telecommunication window, we used the marked holes around the L4 cavity (that marked in Figure 2), by infiltrating optofluidic materials into them.

To achieve this result, by viewing the output spectrum after changing the refractive index of marked holes each time, refractive indices of optofluidic

materials were selected in a way that the separated wavelength will not be outside the range of the third telecommunication window.

Table 1 shows the results of using optofluidic materials with different refractive indices. According to this table, by infiltration of the optofluidic materials with refractive indices in the range of 1.3 to 1.5, the output spectrum was in the third telecommunication window range, with the high transmission efficiency.

TABLE 1
Results of using different refractive indices in the marked holes.

n	(λ_0 nm)	Transmission (%)
1.2	Several	≤ 15
1.3	1551	76
1.4	1561	100
1.5	1572	97
1.6	1584	88

3. SIMULATION AND RESULTS

The FDTD method was used to analyze the proposed photonic crystal filter. Therefore, by considering the effective refractive index for the structure and applying the perfectly matched layer boundary condition (PML), the calculations have been performed where the meshing around the structure issue was considered in the x-z plane. The space steps x and z in the FDTD mesh had been chosen equal to $\Delta x = \Delta z = a/16 = 26.37nm$, and the time steps were obtained from (1).

$$\Delta t \leq \left(\frac{1}{C \sqrt{1/\Delta x^2 + 1/\Delta z^2}} \right) \quad (1)$$

Where C is the velocity of light in free space. The effective parameters on the results of the filters are the central wavelength (λ_0), transmission efficiency, and quality factor (Q). The quality factor can be calculated by (2).

$$Q = \lambda_0 / \Delta \lambda \quad (2)$$

Here $\Delta \lambda$ is the full width at half power of the output.

According to Table 1, for optofluidic materials with refractive indices of 1.3 to 1.5, the output spectrum was in the range of the third telecommunication window. For greater accuracy, the refractive index of the infiltrated holes was

increased each time by step 0.01 and the results are presented in Table 2. It can be seen that the output spectrums of the filter were strongly affected by very small change in the refractive index of the marked infiltrated holes and by increasing the refractive index of the optofluidic material, the resonant wavelength increased, as well.

Figure 5, shows the output spectrum of structure when the source was in the input site and the monitor was in the output site of the circuit (a fluid, for example, acetonitrile has been infiltrated within the marked holes). To this end, the refractive index of the marked infiltrated holes was changed to 1.334 [15].

TABLE 2
The result of refractive index increment of the infiltrated holes, by increasing 0.01 in each step.

n	(λ_0 nm)	Transmission (%)
1.3	1551	76
1.31	1551.5	94
1.32	1552.4	98
1.33	1553.1	99
1.34	1554.4	100
1.35	1555	100
1.36	1556.2	100
1.37	1557.4	100
1.38	1558.1	100
1.39	1559	100
1.4	1561.2	100
1.41	1562.4	100
1.42	1563.3	100
1.43	1564.2	100
1.44	1565	100
1.45	1566.2	100
1.46	1567.1	100
1.47	1568.4	100
1.48	1569.8	99
1.49	1570.1	96
1.5	1572.3	95

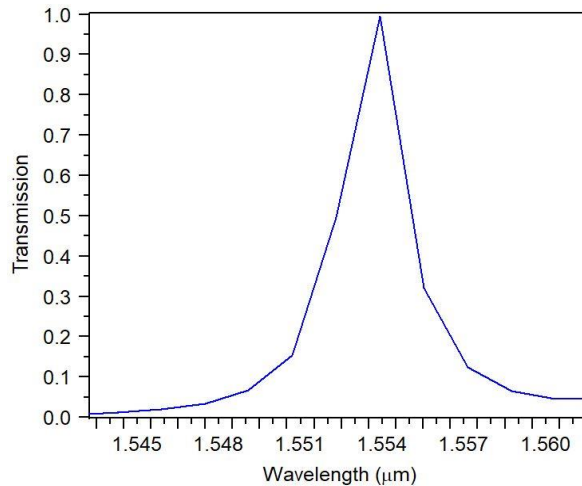


Fig. 5. The output spectrum of structure when acetonitrile has been infiltrated within the marked holes

To observe the performance of the designed filter, several materials such as water, acetonitrile, 1-propanol, and benzene [15] were selected, and the refractive index of the marked infiltrated holes was considered according to the refractive index of these optofluidic materials. The results have been shown in Figure 6 and their properties are listed in Table 3.

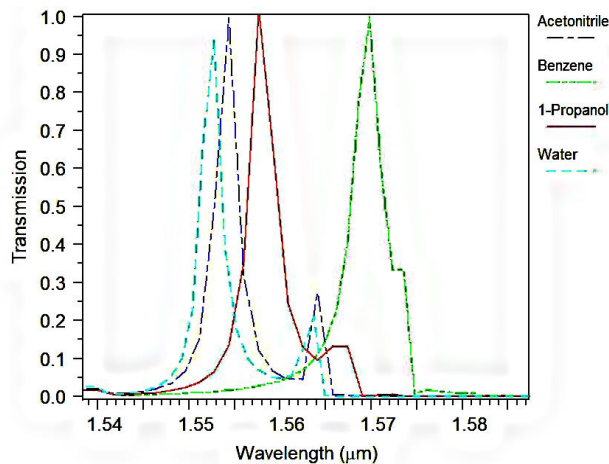


Fig. 6. The output spectrum resulted from the infiltration of the water, acetonitrile, 1-propanol and benzene into the marked holes

TABLE 3

The properties of structure by infiltration of different materials within the marked holes.

Material	n	λ_0 (nm)	Transmission (%)	Q
Water	1.316	1552	94	676.95
Acetonitrile	1.334	1554	99.5	597.8
1-Propanol	1.373	1557	100	523
Benzene	1.478	1569	99.5	250.64

The performance of the filter structure against the input signal was as follows: When the input signals were in the range of resonant cavity wavelengths, for example 1552 nm, it dropped from input to output waveguide (see Figure. 7). When the input signals were in the PBG region, not in the range of resonant cavity wavelengths, for example 1410 nm, the optical signal could not be dropped into the output waveguide (see Figure.8).

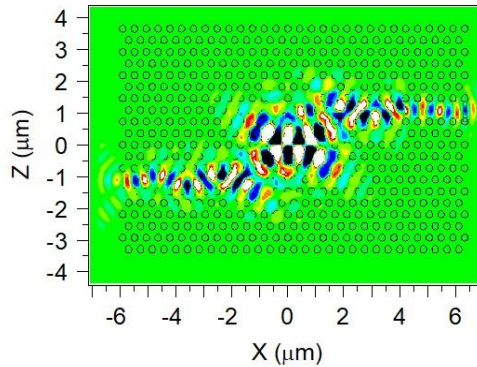


Fig. 7. Propagation of light in the structure with 1552 nm wavelength.

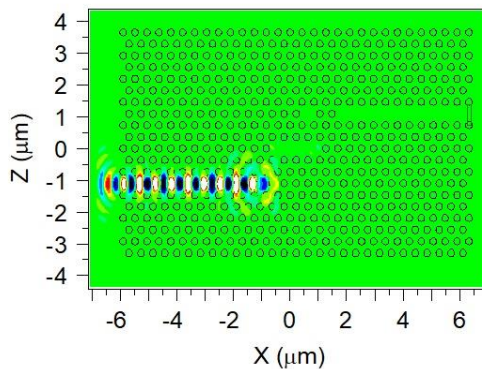


Fig. 8. Propagation of light within PBG region and out of the resonant wavelengths (1410 nm).

The comparison of the properties of the previous works with the proposed structure has been listed in Table 4.

TABLE 4

The comparison of the properties of the previous works with the proposed structure.

Work	Q	Transmission (%)
Ref [4]	221	100
Ref [5]	389	100
Ref [16]	114	100
Ref [17]	344	100
Ref [18]	196	100
Ref [19]	387	90
Ref [20]	114.69	100
Ref [21]	205.5	100
This work (Water)	676.95	94
This work (Acetonitrile)	597.8	99.5
This work (1- propanol)	523	100

4. CONCLUSION

The results showed that the transmission efficiency and the quality factor could be controlled by optofluidic materials that infiltrated within some selected holes. This operation can be done without any change in the radius of holes, which is an important feature of the current design. However, in previously researched works, wavelength separation has already been done by the mechanism of resizing the holes at the nanometer scale and in most of the cases, the fabrication was impossible. Therefore, this work presented a remarkably flexible design in which by changing the optofluidic material, the output wavelength could be easily selected.

REFERENCES

- [1] H. Alipour banaei, F. Mehdizadeh, B. Amini., *All optical communication filter based on photonic crystal structure*, IJFCC, 4(4) (October. 2015) 346–349. <https://doi.org/10.18178/IJFCC.2015.4.5.414>

- [2] M. Seifouri, V. Fallahi, S. Olyaei, *Ultra high-Q optical filter based on photonic crystal ring resonator*, *Photonic Netw Commun*, 35(2) (September. 2018) 225–230. <https://doi.org/10.1007/s11107-017-0732-x>
- [3] K. Zarei, *Investigating the Properties of an optical waveguide based on photonic crystal with point defect and lattice constant perturbation*, *J. Optoelectrical Nanostructures*. 1(1) (Spring. 2016) 1–5. <https://dorl.net/dor/20.1001.1.24237361.2016.1.1.6.3>
- [4] S. Rezaee, M. Zavvari, H. Alipourbanaei, *A novel optical filter based on H-shaped photonic crystal ring resonator*, *Optik*, 126(20) (October. 2015) 2535–2538. <https://doi.org/10.1016/j.ijleo.2015.06.043>
- [5] S. Naghizade, S.M. Sattari-esfahlan, *Excellent quality factor ultra-compact optical communication filter on ring-shaped cavity*, *J. Opt. Commun*, 40(1) (May. 2017) 1–5. <https://doi.org/10.1515/joc-2017-0035>
- [6] F. Mehdizadeh, H. Alipour-banaei, *All optical 1 to 2 decoder based on photonic crystal ring resonator*, *J. Optoelectrical Nanostructures*. 2(2) (Spring.2017) 1–10. <https://dorl.net/dor/20.1001.1.24237361.2017.2.2.1.7>
- [7] B. Elyasi, S. Javahernia, *All optical digital multiplexer using nonlinear photonic crystal ring resonators*, *J. Optoelectrical Nanostructures*. 7(1) (Winter. 2022) 97–106. <https://dorl.net/dor/10.30495/JOPN.2022.29174.1242>
- [8] V. Fallahi, M. Seifouri, *Novel four-channel all optical demultiplexer based on square PCRR for using WDM applications*, *J. Optoelectrical Nanostructures*. 3(4) (Autumn. 2018). <https://dorl.net/dor/20.1001.1.24237361.2018.3.4.5.2>
- [9] K. Venkatachalam, D.S. Kumar, S. Robinson., *Investigation on 2D photonic crystal based eight-channel wavelength-division demultiplexer*, *Photonic Netw Commun*, 34(1) (November. 2016) 100–110. <https://doi.org/10.1007/s11107-016-0675-7>
- [10] Z. Rashki, *Novel design for photonic crystal ring resonators based optical channel drop filter*, *J. Optoelectrical Nanostructures*. 3(3) (Summer. 2018) 59–78. <https://dorl.net/dor/20.1001.1.24237361.2018.3.3.6.1>
- [11] A. Vaisi, M. Soroosh, A. Mahmoudi, *Low loss and high-quality factor optical filter using photonic crystal-based resonant cavity*, *J. Opt. Commun*, 39(3) (June. 2018) 285–288. <https://doi.org/10.1515/joc-2016-0135>

- [12] S.G. Johnson, JD. Joannopoulos, *Block-iterative frequency-domain methods for Maxwell's equations in a plane wave basis*, Opt. Express, 8(3) (January. 2001) 173–190. <https://doi.org/10.1364/OE.8.000173>
- [13] K. Venkatachalam D. Sriram Kumar S. Robinson, *Performance analysis of 2D-Photonic Crystal based Eight Channel Wavelength Division Demultiplexer*, Optik (127)(20) (October. 2016) 8819-8826. <https://doi.org/10.1016/j.ijleo.2016.06.112>
- [14] RSoft software, available at: www.synopsys.com/photonic-solutions/rsoft-photonic-device-tools/rsoft-products.html, (accessed 1 June 2022).
- [15] E. John, S. Aunders, C. Sanders, H. P. Loock *Refractive indices of common solvents and solutions at 1550nm*, applied optics, 55(4) (February. 2016) 947–953. <https://doi.org/10.1364/AO.55.000947>
- [16] S. Robinson, R. Nakkeeran, *Two-dimensional photonic crystal ring resonator based add drop filter for CWDM systems*, Opt Int J Light Electron, 124(18) (September. 2013) 3430-3435. <https://doi.org/10.1016/j.ijleo.2012.10.038>
- [17] F. Mehdizadeh, H. Alipour-Banaei, S. Serajmohammadi, *Channel-drop filter based on a photonic crystal ring resonator*, J. Opt, 15(7) (May. 2013) 1-7. <https://doi.org/10.1088/2040-8978/15/7/075401>
- [18] M. Noori, M., Soroosh, M., Baghban, H.: *All-angle self-collimation in two-dimensional square array photonic crystals based on index contrast tailoring*, Opt Eng, 54(3) (March. 2015) 037111(1-7). <https://doi.org/10.1117/1.oe.54.3.037111>
- [19] H. Alipour-Banaei, M.Jahanara, F. Mehdizadeh, *T-shaped channel drop filter based on photonic crystal ring resonator*, Optik , 125(18) (September. 2014) 5348-5351. <https://doi.org/10.1016/j.ijleo.2014.06.056>
- [20] S. Robinson, R. Nakkeeran, *Coupled mode theory analysis for circular photonic crystal ring resonator-based add-drop filter*, Opt. Eng, 51(11) (November. 2012) 114001(1-6). <https://doi.org/10.1117/1.oe.51.11.114001>
- [21] VR. Balaji, M. Murgan, S.Robinson, *Optimization of DWDM demultiplexer using regression analysis*, J Adv Engg Tech, 2016 (May. 2016) 1-10. <https://doi.org/10.1155/2016/9850457>